Supporting Information

UV/Vis and Fluorescence Spectra, Stability

Py-NMe$_2$

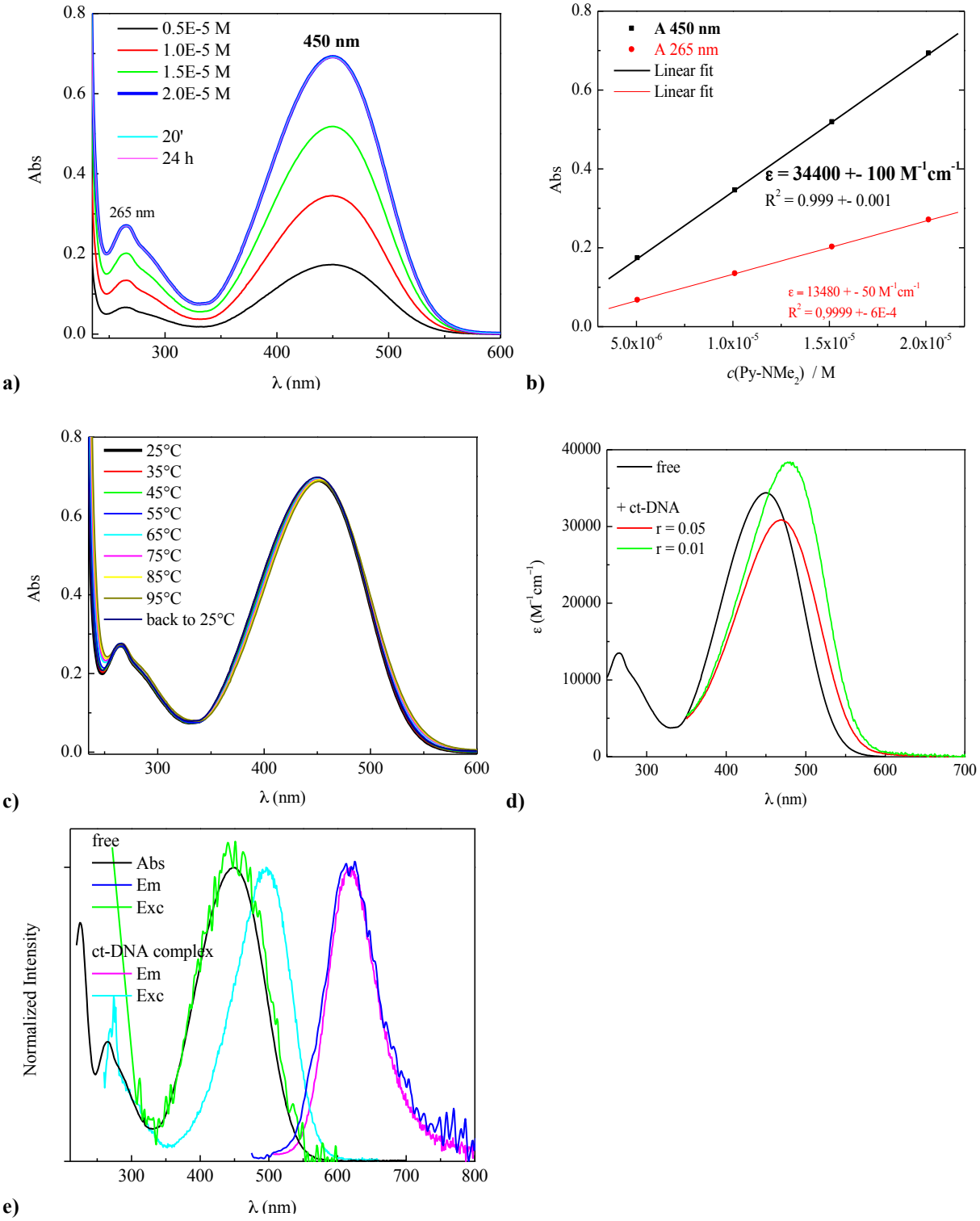

Figure S1. a) Concentration dependence of the UV-Vis spectrum of **Py-NMe$_2$** (concentration range 5 – 20 µM); **b)** Molar extinction coefficients (ε) at Absorption maxima; **c)** Temperature dependence of the UV-Vis spectrum of **Py-NMe$_2$** (c = 20 µM); **d)** Spectral shift upon addition of ct-DNA; **e)** Overlayed normalized spectra of the free compound and ct-DNA complex: Absorption, Emission and Excitation. pH 7, sodium cacodylate buffer, I = 0.05 M.

Q-NMe$_2$

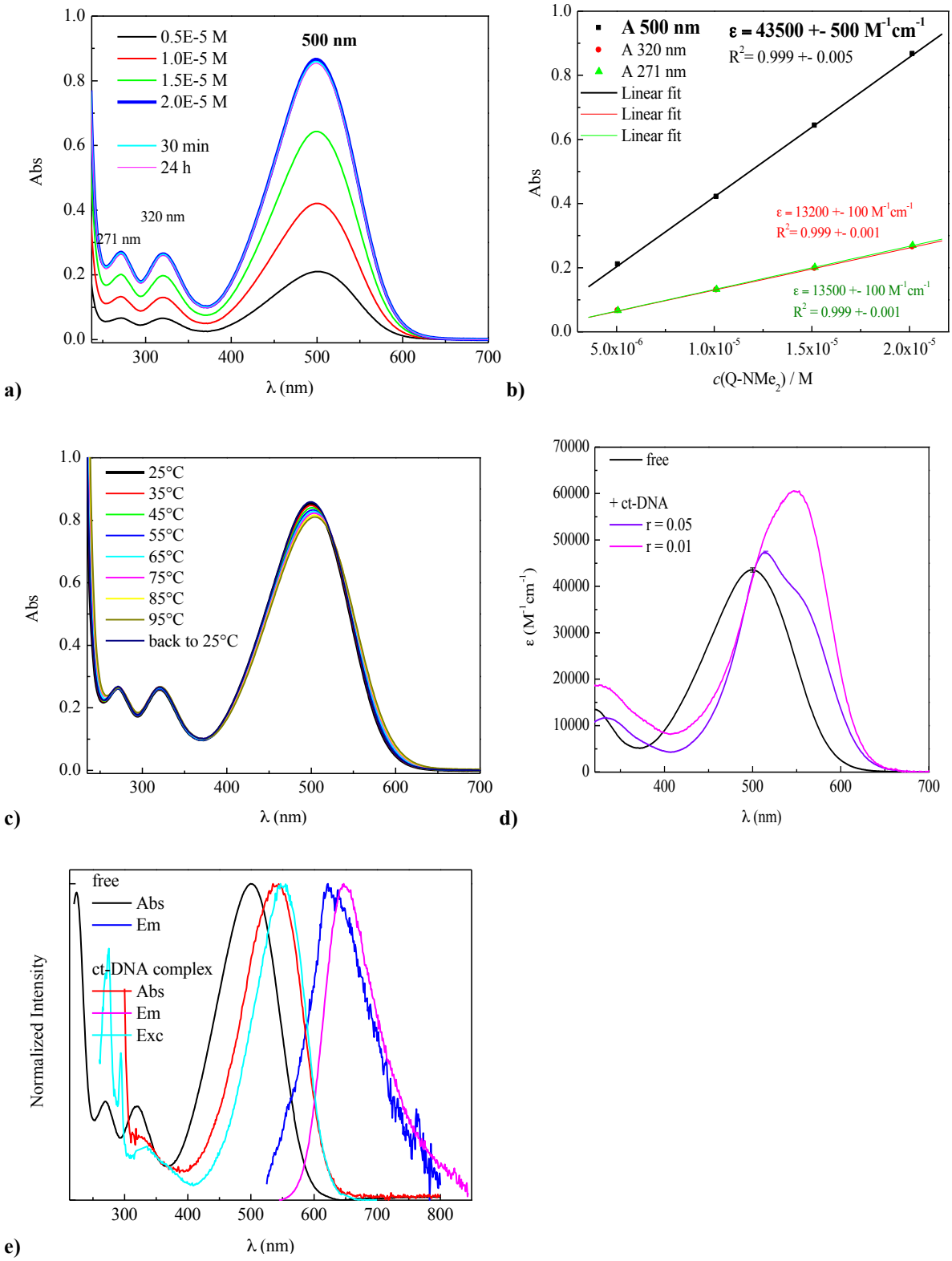

Figure S2. a) Concentration dependence of the UV-Vis spectrum of **Q-NMe$_2$** (concentration range 5 – 20 μM); **b)** Molar extinction coefficients (ε) at Absorption maxima; **c)** Temperature dependence of the UV-Vis spectrum of **Q-NMe$_2$** (c = 20 μM); **d)** Spectral shift upon addition of ct-DNA; **e)** Overlayed normalized spectra of the free compound and ct-DNA complex: Absorption, Emission and Excitation. pH 7, sodium cacodylate buffer, I = 0.05 M.

Q-NPh$_2$

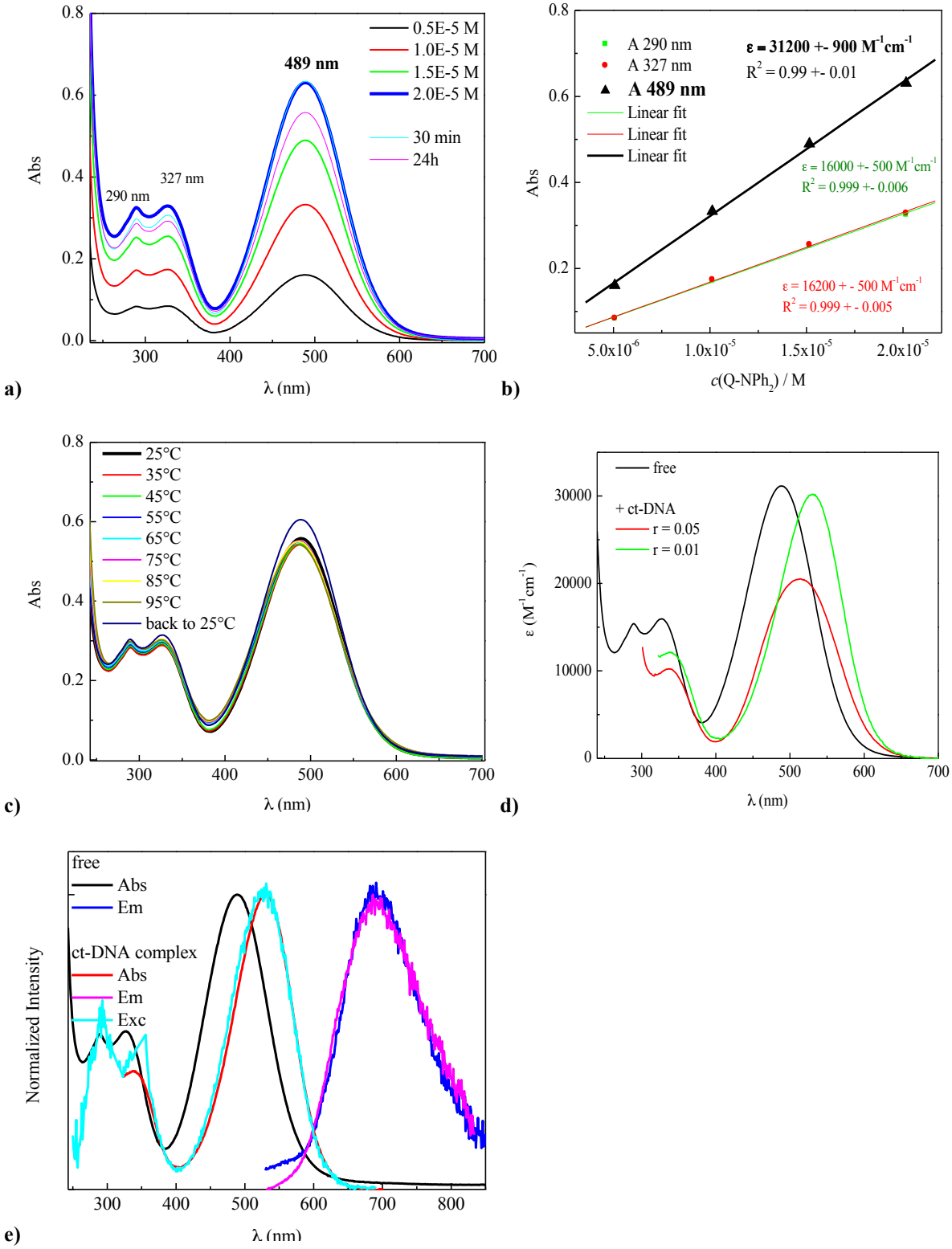

Figure S3. a) Concentration dependence of the UV-Vis spectrum of **Q-NPh$_2$** (concentration range 5 – 20 µM); **b)** Molar extinction coefficients (ε) at Absorption maxima; **c)** Temperature dependence of the UV-Vis spectrum of **Q-NPh$_2$** (c = 20 µM); **d)** Spectral shift upon addition of ct-DNA; **e)** Overlayed normalized spectra of the free compound and ct-DNA complex: Absorption, Emission and Excitation. pH 7, sodium cacodylate buffer, I = 0.05 M.

***p*Py-MeO-*p*Py**

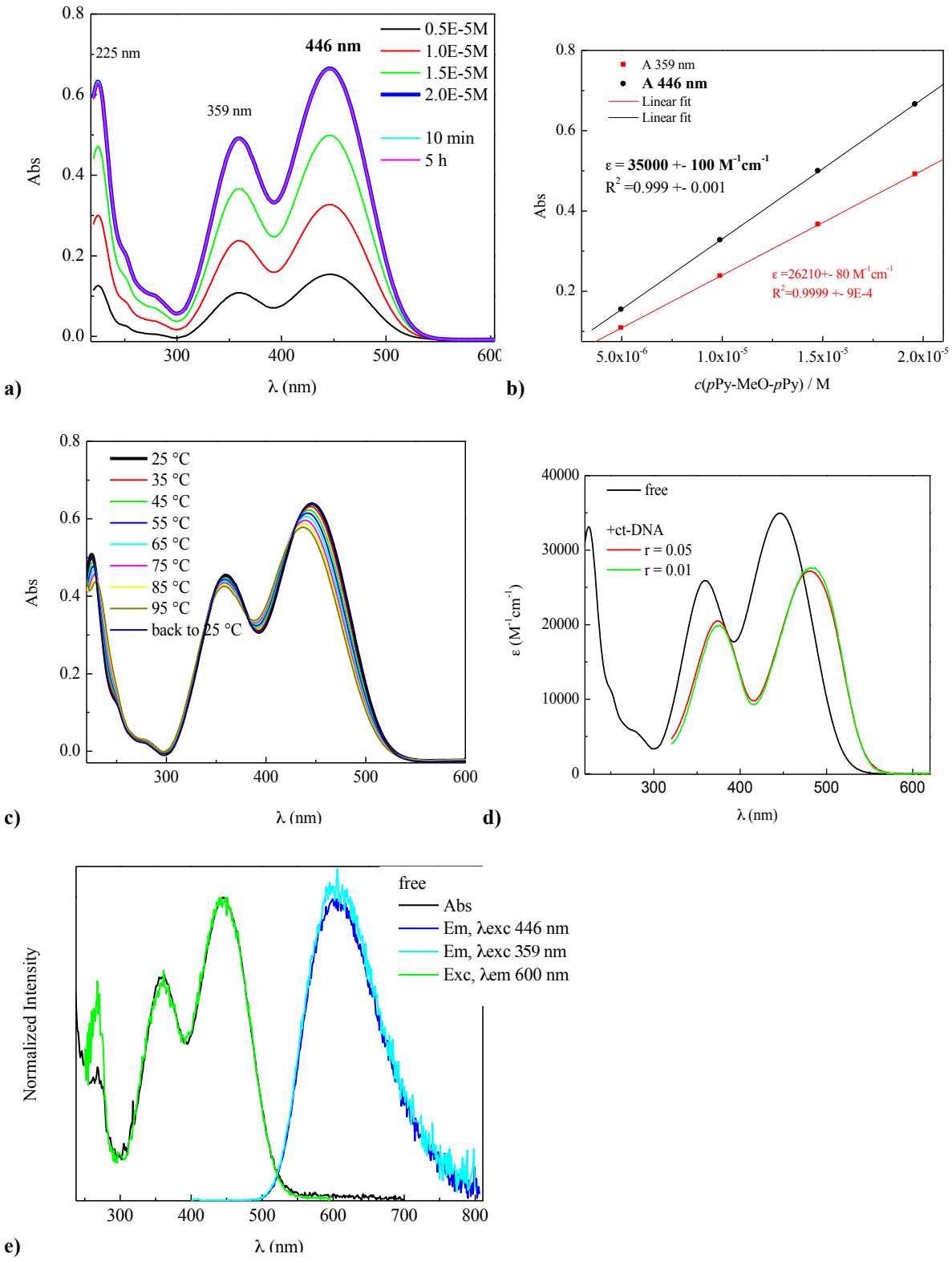

Figure S4. a) Concentration dependence of the UV-Vis spectrum of ***p*Py-MeO-*p*Py** (concentration range 5 – 20 µM); **b)** Molar extinction coefficients (ε) at Absorption maxima; **c)** Temperature dependence of the UV-Vis spectrum of ***p*Py-MeO-*p*Py** (c = 20 µM); **d)** Spectral shift upon addition of ct-DNA; **e)** Overlayed normalized spectra of the free compound: Absorption, Emission and Excitation. pH 7, sodium cacodylate buffer, I = 0.05 M.

***o*Py-MeO-*o*Py**

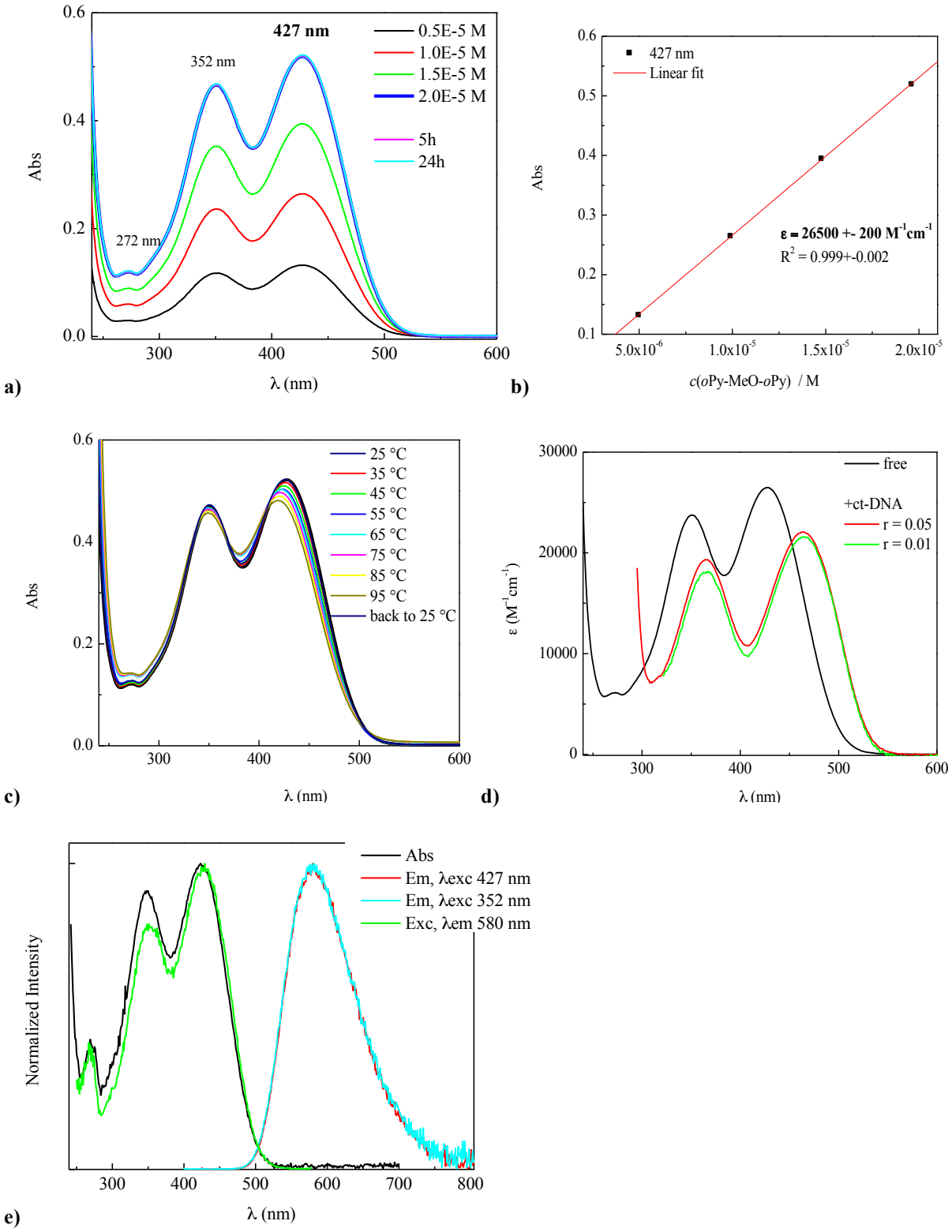

Figure S5. a) Concentration dependence of the UV-Vis spectrum of ***o*Py-MeO-*o*Py** (concentration range 5 – 20 µM); **b)** Molar extinction coefficients (ε) at Absorption maxima; **c)** Temperature dependence of the UV-Vis spectrum of ***o*Py-MeO-*o*Py** (c = 20 µM); **d)** Spectral shift upon addition of ct-DNA; **e)** Overlayed normalized spectra of the free compound: Absorption, Emission and Excitation. pH 7, sodium cacodylate buffer, I = 0.05 M.

Study of interactions with double-stranded DNA/RNA in aqueous medium

Table S1. Structural properties of studied DNA and RNA.[1]

Structure type	Groove width [Å]		Groove depth [Å]	
	major	minor	major	minor
Poly A – poly U	3.8	10.9	-	-
[a]B-DNA (like ct-DNA)	11.7	5.7	8.5	7.5
Poly dGdC – poly dGdC	13.5	9.5	10.0	7.2
Poly dAdT – poly dAdT	11.2	6.3	-	-

[a] Calf Thymus (ct)-DNA

Table S2. Spectral shifts of ***p*Py-MeO-*p*Py** and ***o*Py-MeO-*o*Py** upon binding dsDNAs/RNA at r (compound/polynucleotide) = 0.05 in buffered solution (pH 7.0, I = 0.05 M).

		λ_{max} (nm)				
		free	**ct-DNA**	**p(dAdT)$_2$**	**p(dGdC)$_2$**	**p(AU)**
***p*Py-MeO-*p*Py**	Abs	359, 446	374, 481 (+35)	477 (+31)	484 (+38)	477 (+31)
	Em	605	591 (-14)	588 (-17)	605 (0)	595 (-13)
	Exc	359, 446	465	468	450	473
***o*Py-MeO-*o*Py**	Abs	352, 427	365, 464 (+37)	460 (+33)	464(+37)	458(+31)
	Em	580	578 (-2)	574 (-6)	582 (+2)	580 (0)
	Exc	427	431	458	426	432

Thermal melting experiments

ΔT_m with **Py-NMe$_2$**

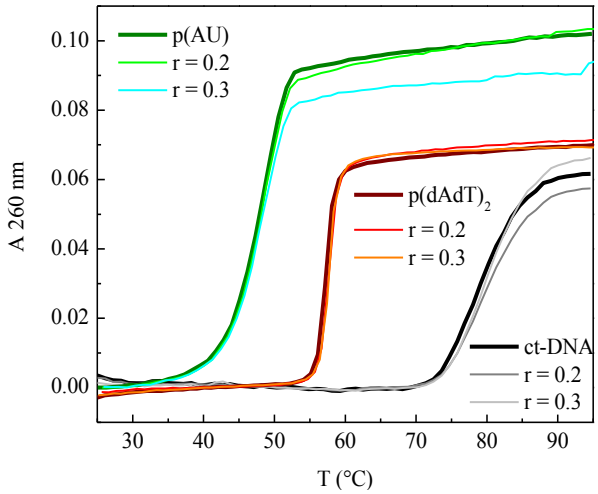

Figure S6. Melting curves of ct-DNA, p(dAdT)$_2$ and p(AU) upon addition of **Py-NMe$_2$** (r = 0.2 and r = 0.3 (c(dye)/c(polynucleotide))) at pH 7.0 (buffer sodium cacodylate, I = 0.05 M).

ΔT_m with **Q-NMe$_2$** and **Q-NPh$_2$**

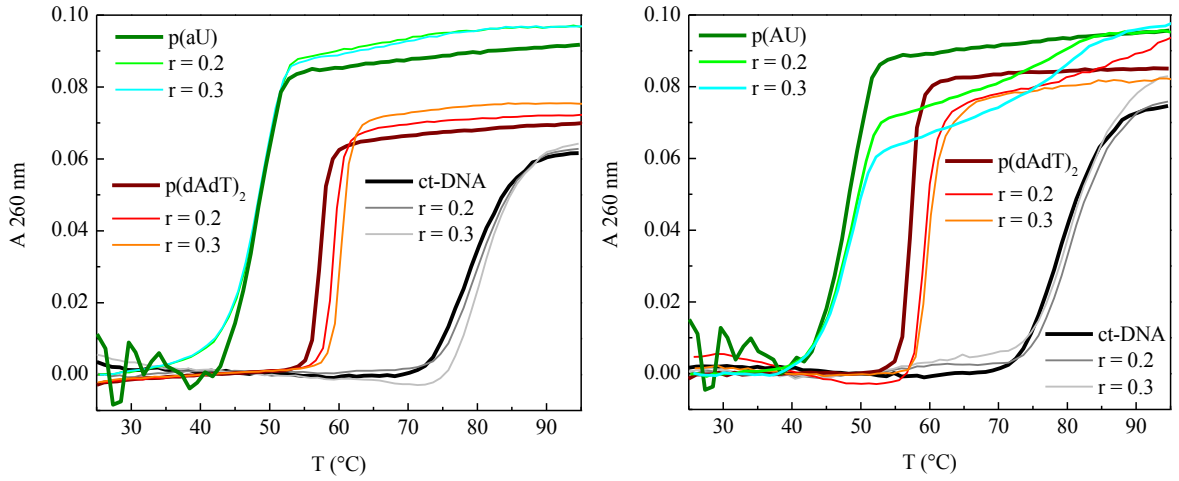

Figure S7. Melting curves of ct-DNA, p(dAdT)$_2$ and p(AU) upon addition of **Q-NMe$_2$** (LEFT**)** and **Q-NPh$_2$** (RIGHT) **(***r* = 0.2 and *r* = 0.3 (*c*(dye)/*c*(polynucleotide)) at pH 7.0 (buffer sodium cacodylate, *I* = 0.05 M).

ΔT_m with ***p*Py-MeO-*p*Py** and ***o*Py-MeO-*o*Py**

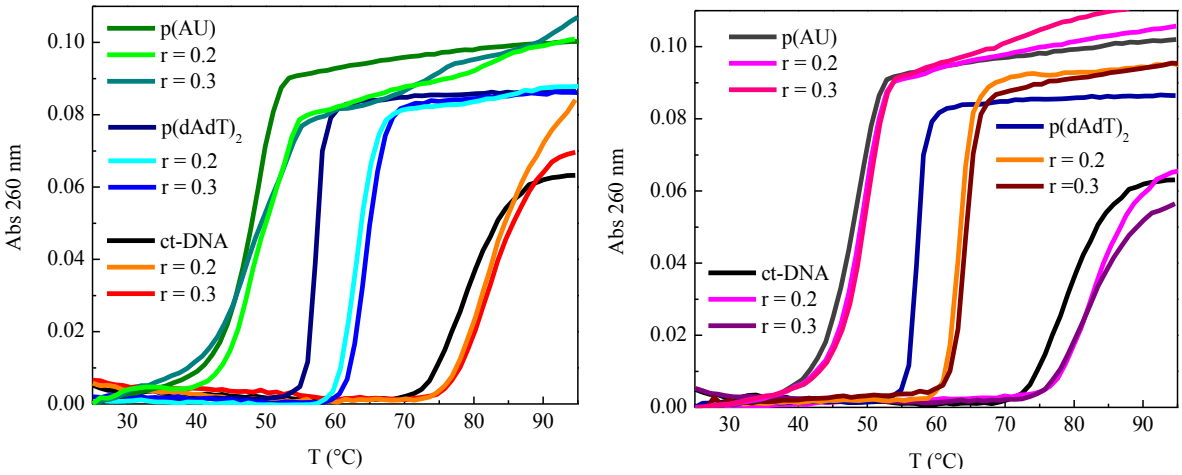

Figure S8. Melting curve of ct-DNA, p(dAdT)$_2$ and p(AU) upon addition of ***p*Py-MeO-*p*Py** (LEFT**)** and ***o*Py-MeO-*o*Py** (RIGHT) **(**r = 0.1 and r = 0.2 (*c*(dye)/*c*(polynucleotide))) at pH 7.0 (buffer sodium cacodylate, *I* = 0.05 M).

Fluorescence Spectrophotometric titrations

Fluorimetric titrations with ***Py-NMe$_2$***

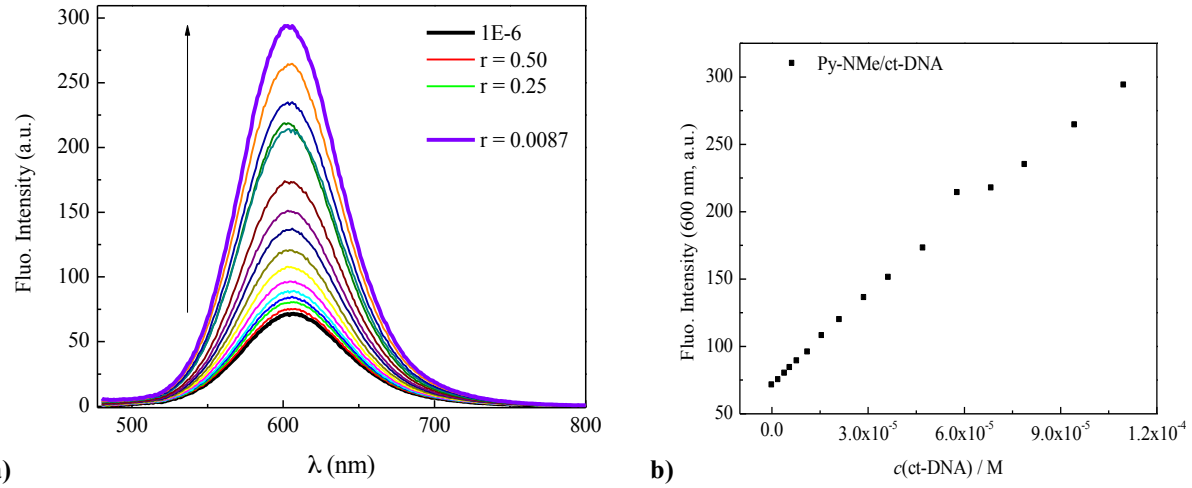

Figure S9. a) Changes in the fluorescence spectrum of ***Py-NMe$_2$*** (λ_{exc} = 450 nm, c = 1 μM), upon titration with ct-DNA; **b)** Dependence of ***Py-NMe$_2$*** fluorescence at λ_{max} on c(ct-DNA). pH 7, sodium cacodylate buffer, I = 0.05 M.

Fluorimetric titrations with **Q-NMe$_2$**

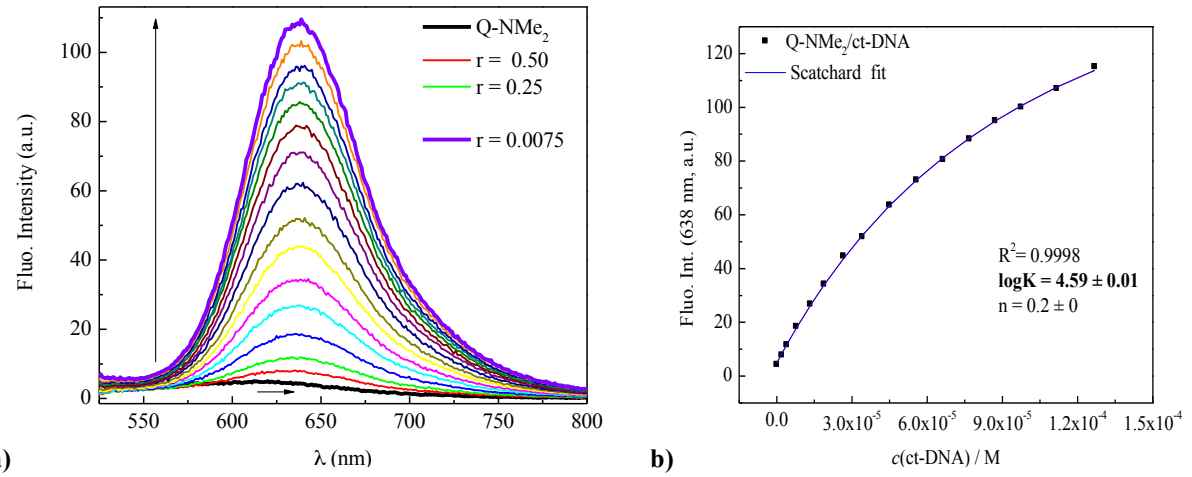

Figure S10. a) Changes in the fluorescence spectrum of **Q-NMe$_2$** (λ_{exc} = 500 nm, c = 1 μM), upon titration with ct-DNA; **b)** Dependence of **Q-NMe$_2$** fluorescence at λ_{max} on c(ct-DNA). pH 7, sodium cacodylate buffer, I = 0.05 M.

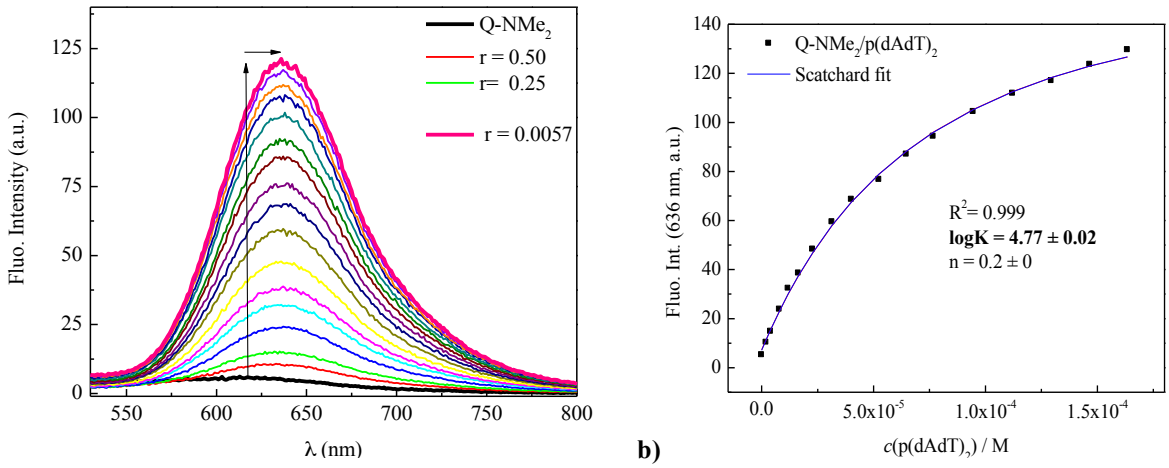

Figure S11. a) Changes in the fluorescence spectrum of **Q-NMe$_2$** (λ_{exc} = 500 nm, c = 1 μM), upon titration with p(dAdT)$_2$; **b)** Dependence of **Q-NMe$_2$** fluorescence at λ_{max} on c(p(dAdT)$_2$). pH 7, sodium cacodylate buffer, I = 0.05 M.

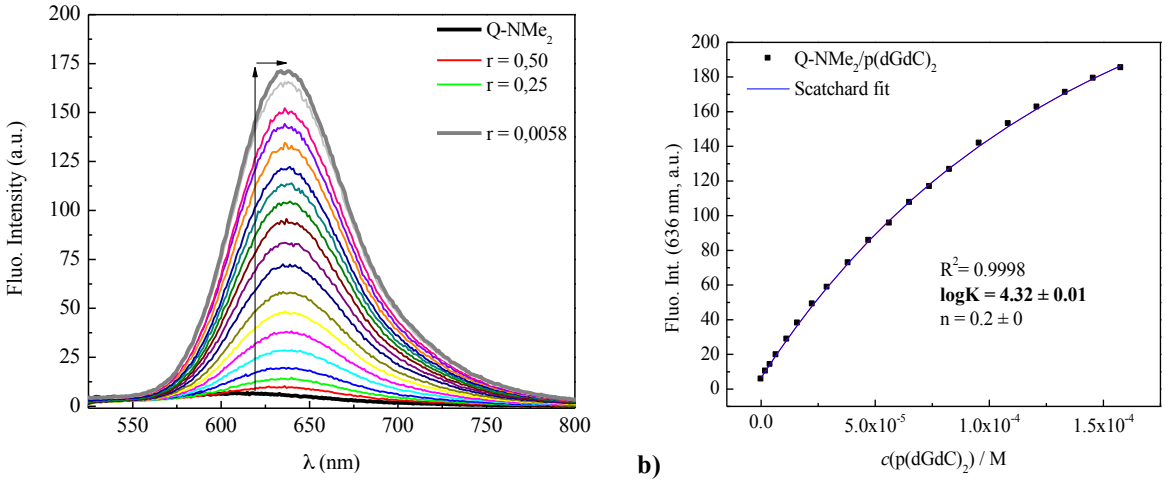

Figure S12. a) Changes in the fluorescence spectrum of **Q-NMe$_2$** (λ_{exc} = 500 nm, c = 1 μM), upon titration with p(dGdC)$_2$; **b)** Dependence of **Q-NMe$_2$** fluorescence at λ_{max} on c(p(dGdC)$_2$). pH 7, sodium cacodylate buffer, I = 0.05 M.

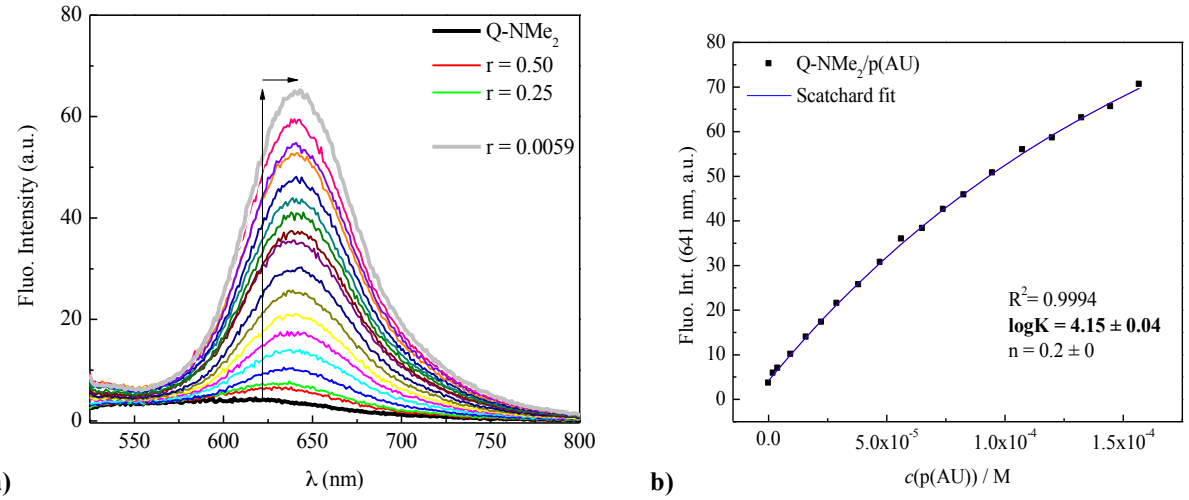

Figure S13. a) Changes in the fluorescence spectrum of **Q-NMe$_2$** (λ_{exc} = 500 nm, c = 1 μM), upon titration with p(AU); **b)** Dependence of **Q-NMe$_2$** fluorescence at λ_{max} on c(p(AU)). pH 7, sodium cacodylate buffer, I = 0.05 M.

Fluorimetric titrations with **Q-NPh$_2$**

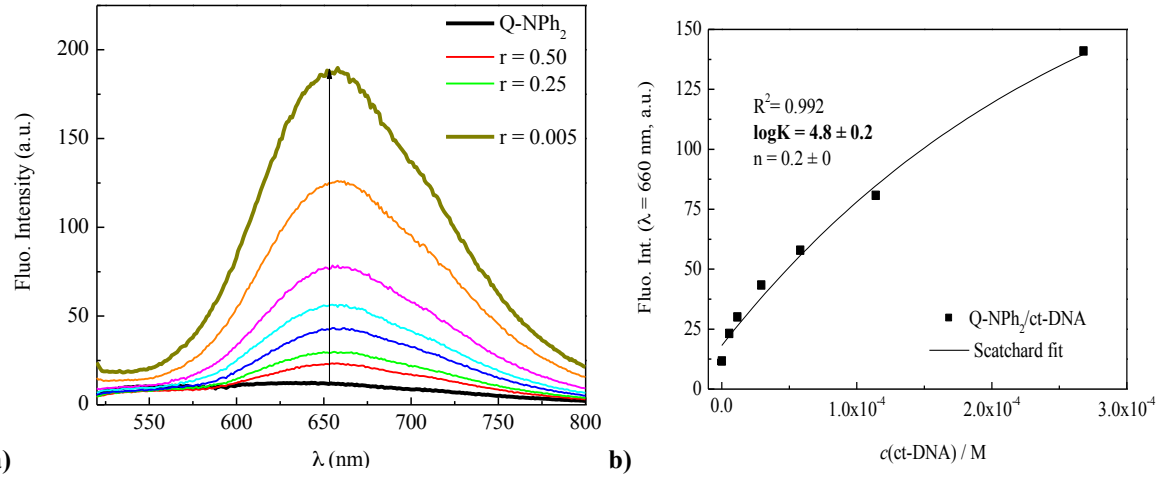

Figure S14. a) Changes in the fluorescence spectrum of **Q-NPh$_2$** (λ_{exc} = 489 nm, c = 3 μM), upon titration with ct-DNA; **b)** Dependence of **Q-NPh$_2$** fluorescence at λ_{max} on c(ct-DNA). pH 7, sodium cacodylate buffer, I = 0.05 M.

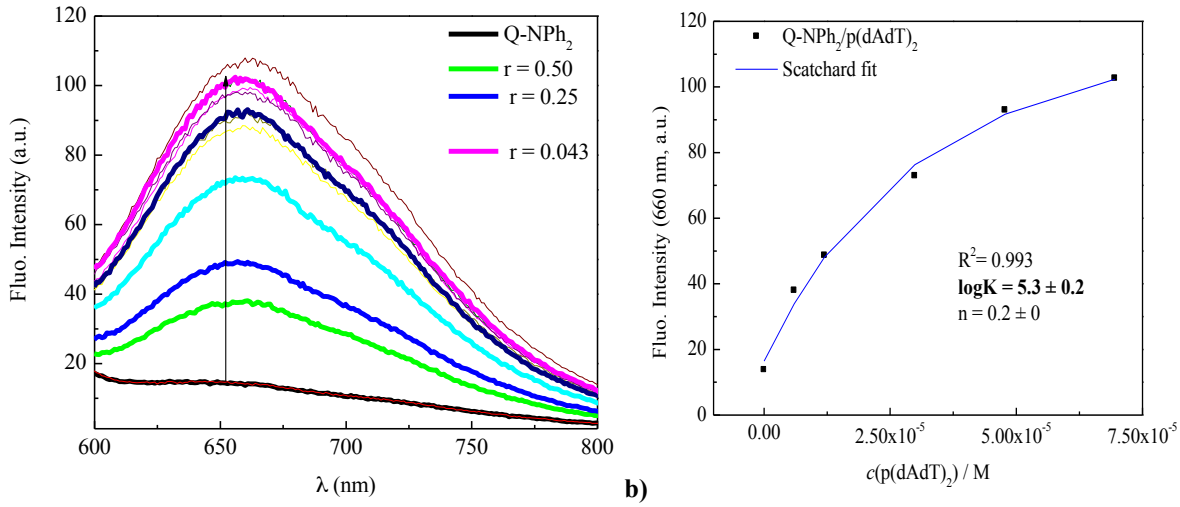

Figure S15. a) Changes in thefluorescence spectrum of **Q-NPh$_2$** (λ_{exc} = 489 nm, c = 3 μM), upon titration with p(dAdT)$_2$; **b)** Dependence of **Q-NPh$_2$** fluorescence at λ_{max} on c(p(dAdT)$_2$). Done at pH 7, sodium cacodylate buffer, I = 0.05 M.

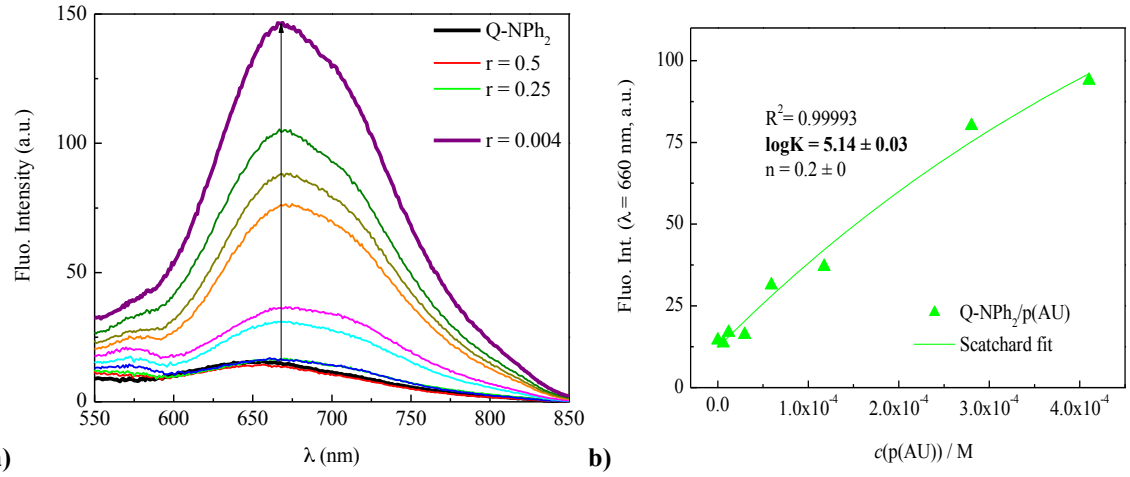

Figure S16. a) Changes in the fluorescence spectrum of **Q-NPh$_2$** (λ_{exc} = 489 nm, c = 3 μM), upon titration with p(AU); **b)** Dependence of **Q-NPh$_2$** fluorescence at λ_{max} on c(p(AU)). pH 7, sodium cacodylate buffer, I = 0.05 M.

Fluorimetric titrations with ***p*Py-MeO-*p*Py**

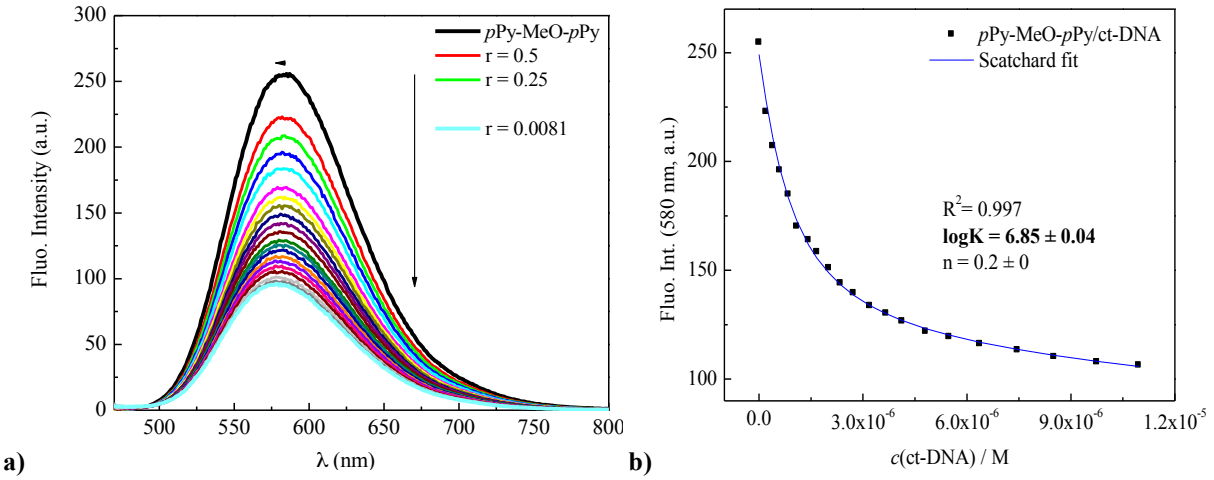

Figure S17. a) Changes in the fluorescence spectrum of ***p*Py-MeO-*p*Py** (λ_{exc} = 445 nm, c = 0.1 μM), upon titration with ct-DNA; **b)** Dependence of ***p*Py-MeO-*p*Py** fluorescence at λ_{max} on c(ct-DNA). pH 7, sodium cacodylate buffer, I = 0.05 M.

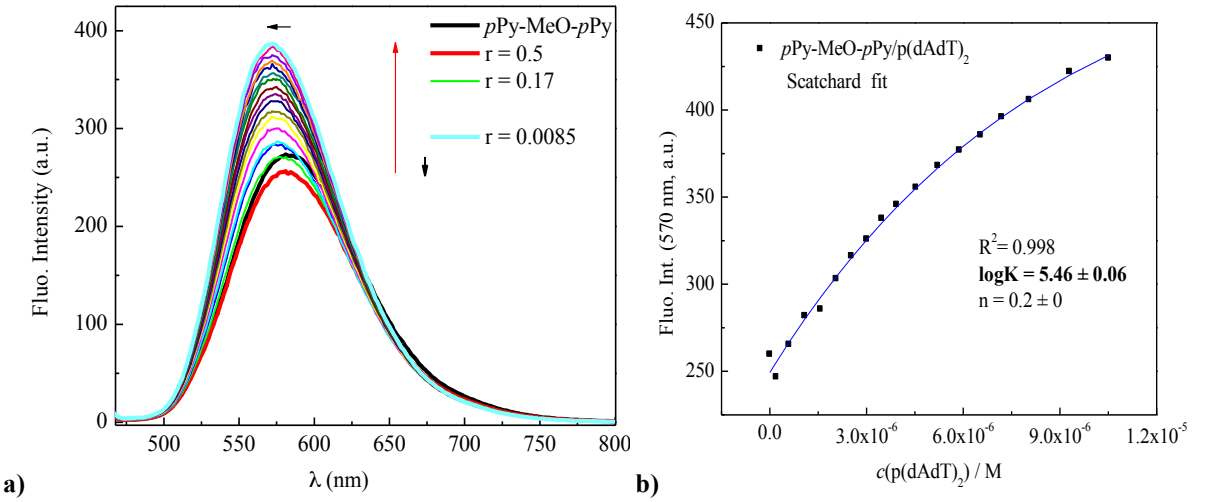

Figure S18. a) Changes in the fluorescence spectrum of ***p*Py-MeO-*p*Py** (λ_{exc} = 445 nm, c = 0.1 μM), upon titration with p(dAdT)$_2$; **b)** Dependence of ***p*Py-MeO-*p*Py** fluorescence at λ_{max} on c(p(dAdT)$_2$). pH 7, sodium cacodylate buffer, I = 0.05 M.

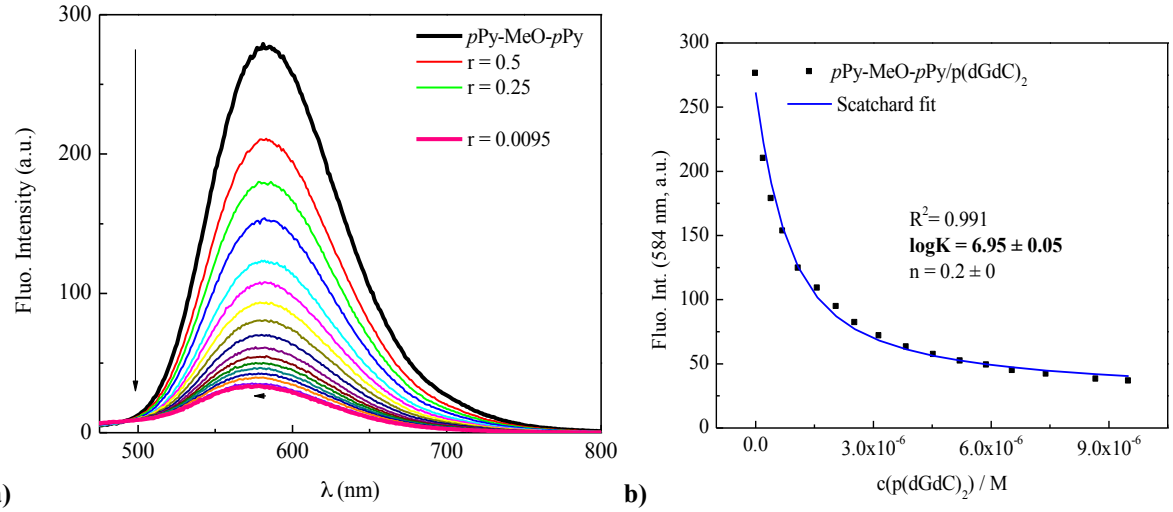

Figure S19. a) Changes in the fluorescence spectrum of ***p*Py-MeO-*p*Py** (λ_{exc} = 445 nm, c = 0.1 μM), upon titration with p(dGdC)$_2$; **b)** Dependence of ***p*Py-MeO-*p*Py** fluorescence at λ_{max} on c(p(dGdC)$_2$). pH 7, sodium cacodylate buffer, I = 0.05 M.

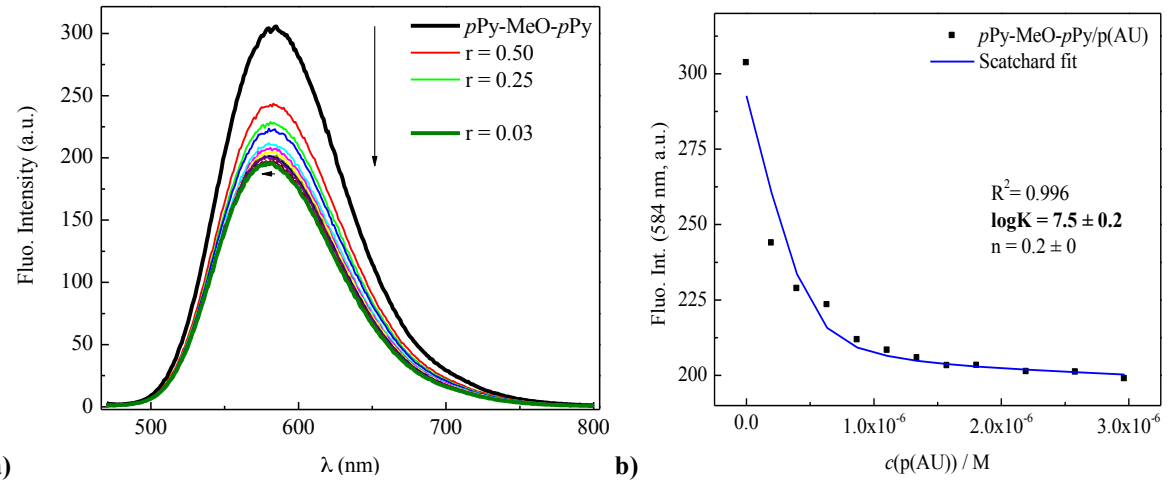

Figure S20. a) Changes in the fluorescence spectrum of ***p*Py-MeO-*p*Py** (λ_{exc} = 445 nm, c = 0.1 μM), upon titration with p(AU); **b)** Dependence of ***p*Py-MeO-*p*Py** fluorescence at λ_{max} on c(p(AU)). pH 7, sodium cacodylate buffer, I = 0.05 M.

Fluorimetric titrations with ***o*Py-MeO-*o*Py**

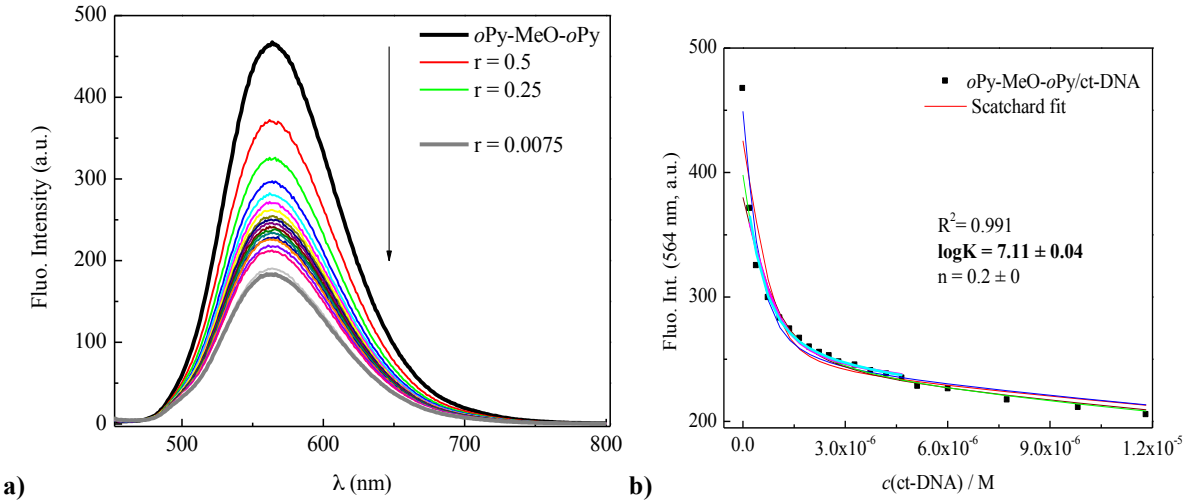

Figure S21. a) Changes in the fluorescence spectrum of ***o*Py-MeO-*o*Py** (λ_{exc} = 427 nm, c = 0.1 μM), upon titration with ct-DNA; **b)** Dependence of ***o*Py-MeO-*o*Py** fluorescence at λ_{max} on c(ct-DNA). pH 7, sodium cacodylate buffer, I = 0.05 M.

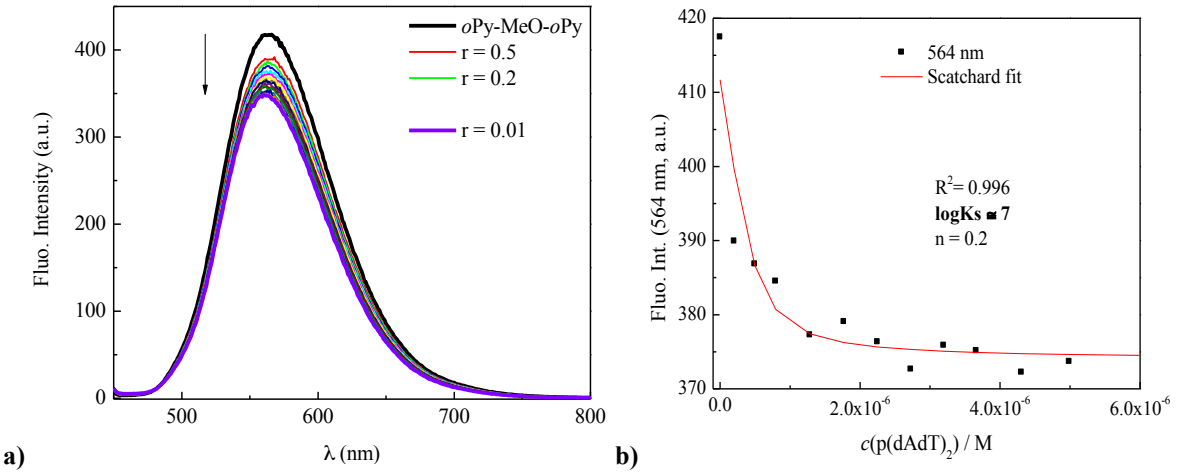

Figure S22. a) Changes in the fluorescence spectrum of ***o*Py-MeO-*o*Py** (λ_{exc} = 427 nm, c = 0.1 μM), upon titration with p(dAdT)$_2$; **b)** Dependence of ***o*Py-MeO-*o*Py** intensity at λmax on c(p(dA-dT)$_2$). pH 7.0, sodium cacodylate buffer, I = 0.05 M.

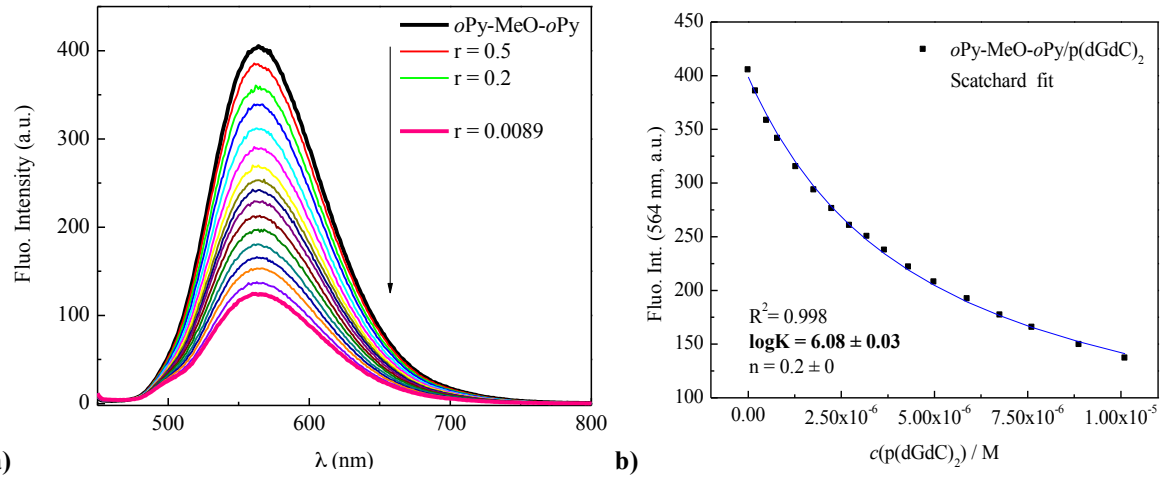

Figure S23. a) Changes in the fluorescence spectrum of ***o*Py-MeO-*o*Py** (λ_{exc} = 427 nm, c = 0.1 μM), upon titration with p(dGdC)$_2$; **b)** Dependence of ***o*Py-MeO-*o*Py** fluorescence at λ_{max} on c(p(dGdC)$_2$). pH 7, sodium cacodylate buffer, I = 0.05 M.

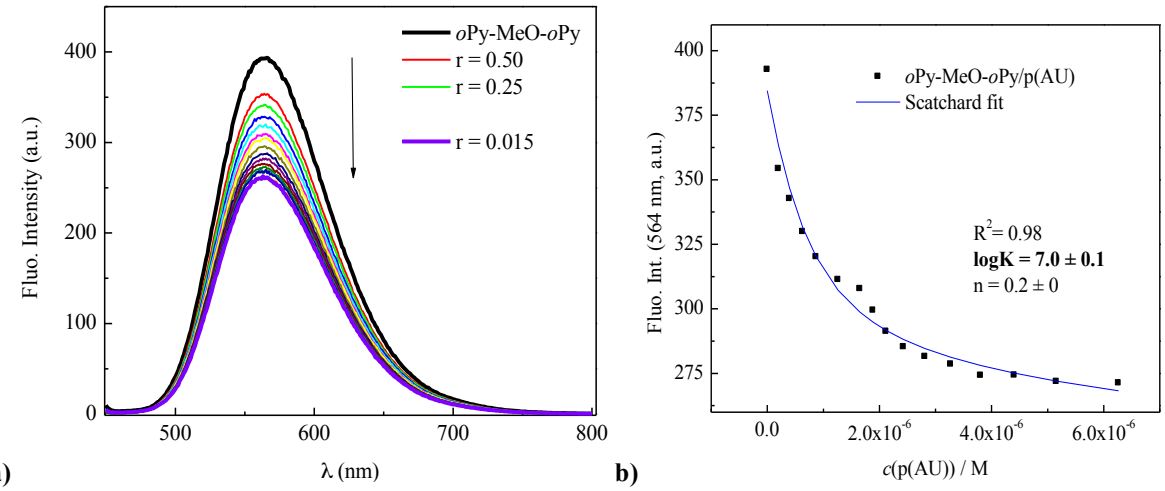

Figure S24. a) Changes in the fluorescence spectrum of ***o*Py-MeO-*o*Py** (λ_{exc} = 427 nm, c = 0.1 μM), upon titration with p(AU); **b)** Dependence of ***o*Py-MeO-*o*Py** fluorescence at λ_{max} on c(p(AU)). pH 7, sodium cacodylate buffer, I = 0.05 M.

CD experiments

CD titrations of ds DNAs/RNA with **Py-NMe$_2$**

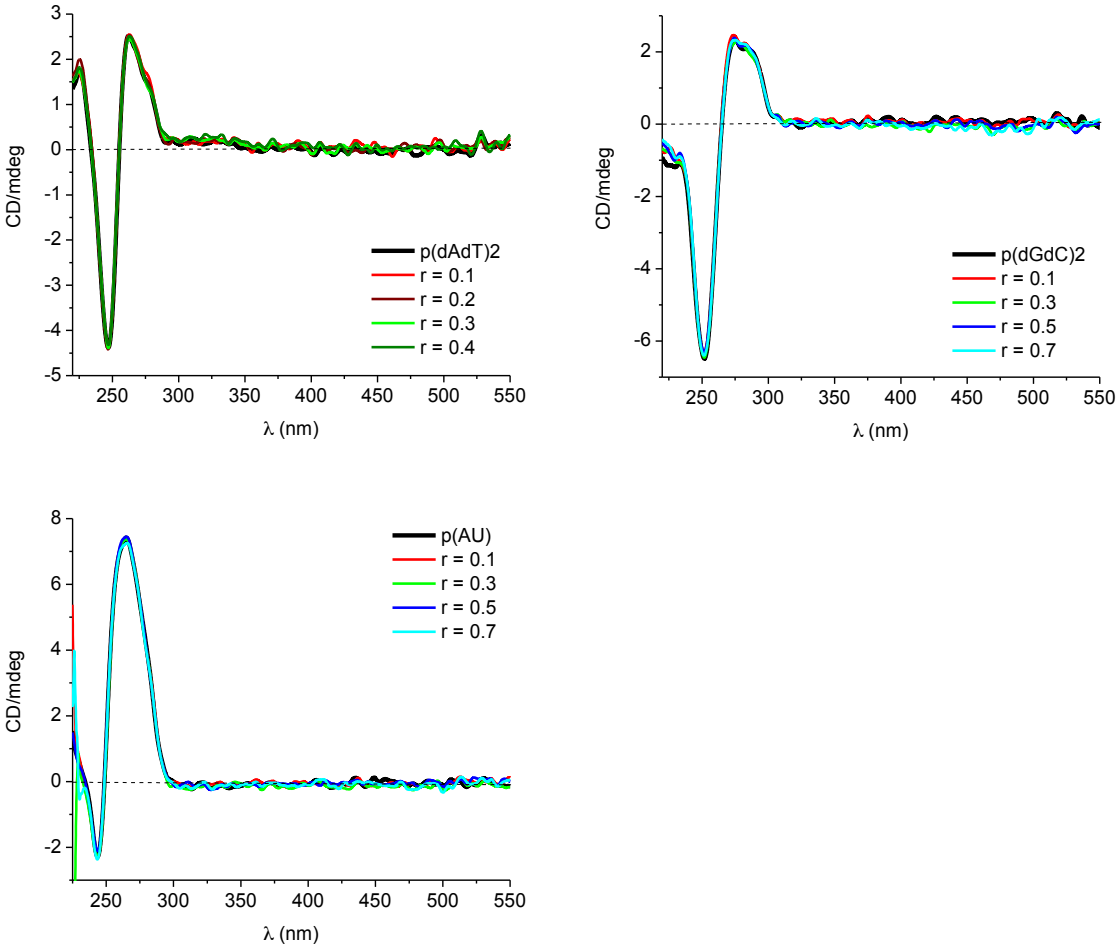

Figure S25. CD titration of p(dAdT)$_2$, p(dGdC)$_2$ and p(AU) (all DNA and RNA c = 20 μM) with **Py-NMe$_2$** at molar ratios r = [compound] / [polynucleotide] = 0.1 – (0.4) 0.7; (pH 7.0, buffer sodium cacodylate, I = 0.05 M).

Time-Resolved (Single-Photon Counting and Transient Absorption) Spectroscopic Techniques

TC-Single-Photon Counting with **Py-NMe$_2$**

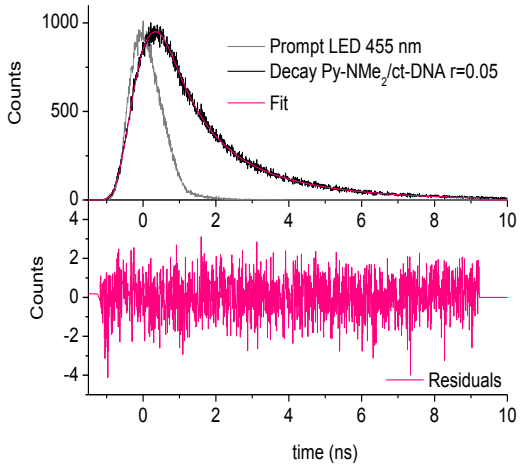

Figure S26. TC-SPC Fluorescence Decay of **Py-NMe$_2$** complexed with ct-DNA r (*c*(dye)/*c*(polynucleotide)) = 0.05 in pH 7.0, buffer sodium cacodylate, I = 0.05 M.

TC-Single-Photon Counting with ***p*Py-MeO-*p*Py** and ***o*Py-MeO-*o*Py**

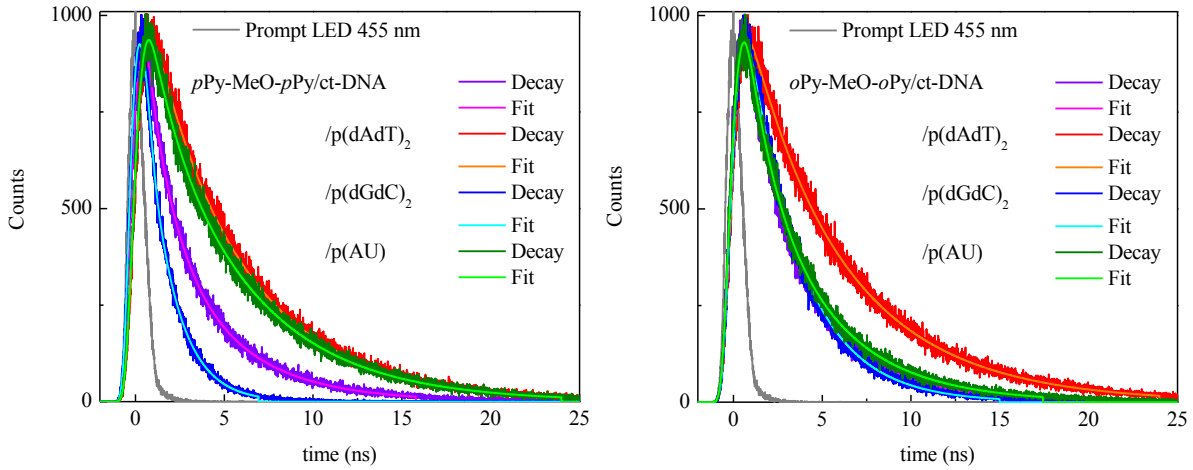

Figure S27. TC-SPC Fluorescence Decays of ***p*Py-MeO-*p*Py** (LEFT) and ***o*Py-MeO-*o*Py** (RIGHT) complexed with dsDNAs/RNA r (*c*(dye)/*c*(polynucleotide)) = 0.05 in pH 7.0, buffer sodium cacodylate, I = 0.05 M.

Transient Absorption

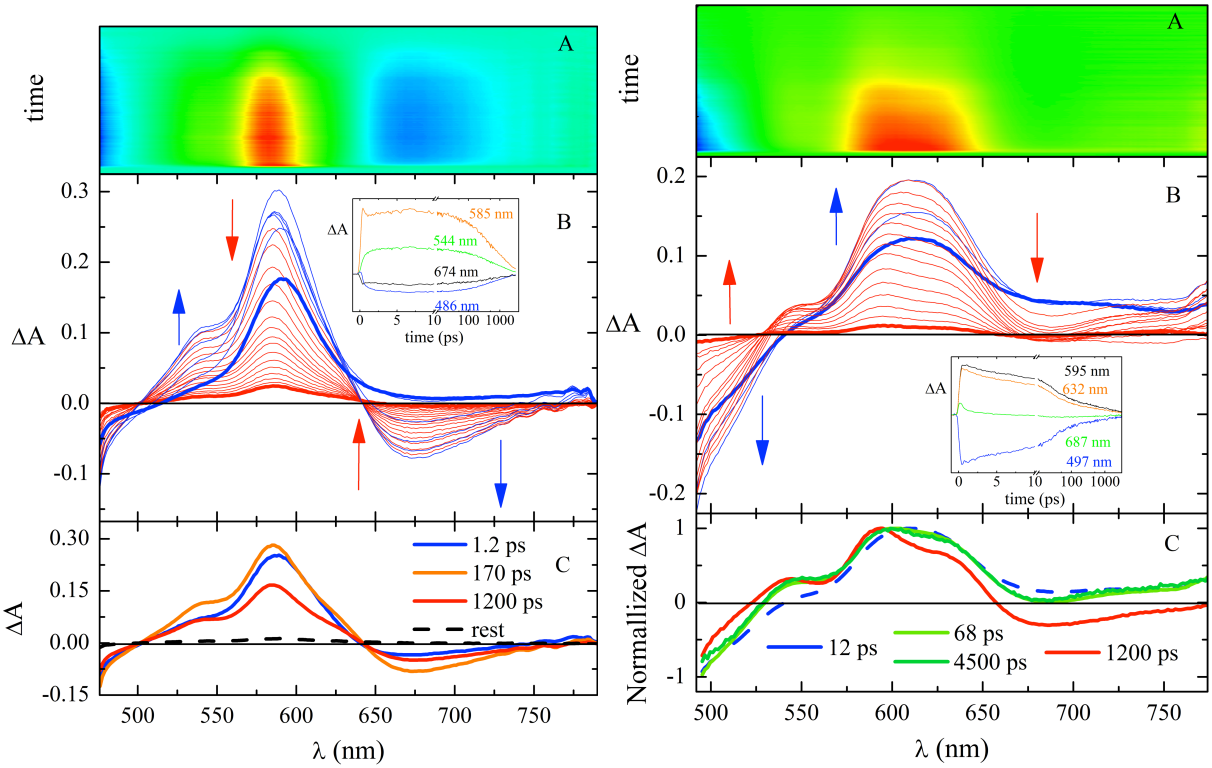

Figure S28. Pump−probe absorption spectroscopy of compound ***p*Py-MeO-*p*Py** in water (LEFT), complexed with ct-DNA in buffer solution at r (*c*(dye)/*c*(ct-DNA)) =0.05 (RIGHT), (λ_{exc} = 400 nm): (**A**) contour plot of the experimental data, (**B**) time- resolved absorption spectra recorded at different delays after the laser pulse (inset: decay kinetics recorded at meaningful wavelengths), and (**C**) species associated spectra obtained by global analysis.

Confocal Microscopy

A)

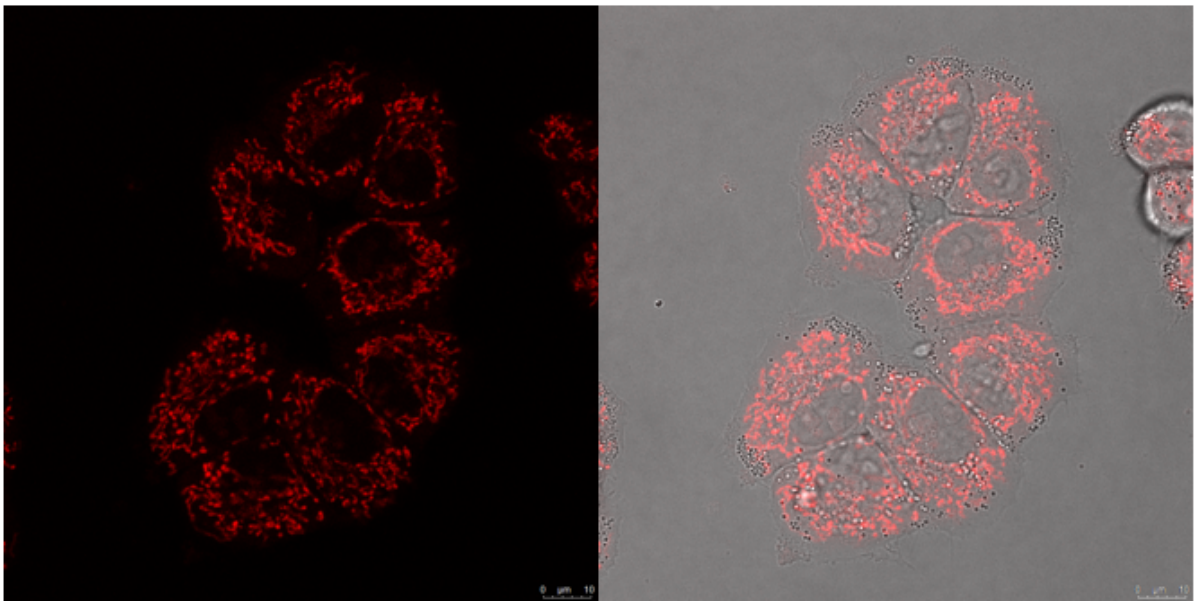

Figure S29.A) LEFT: Confocal microscopy of live cells (*c*=50000 cells/mL) taken on Leica SP8 X confocal microscope, stained with 10 μM concentration of **Py-NMe$_2$** (λ_{exc} = 450 nm, λ_{em} = 605 nm); RIGHT: overlay with the control (white light).

B)

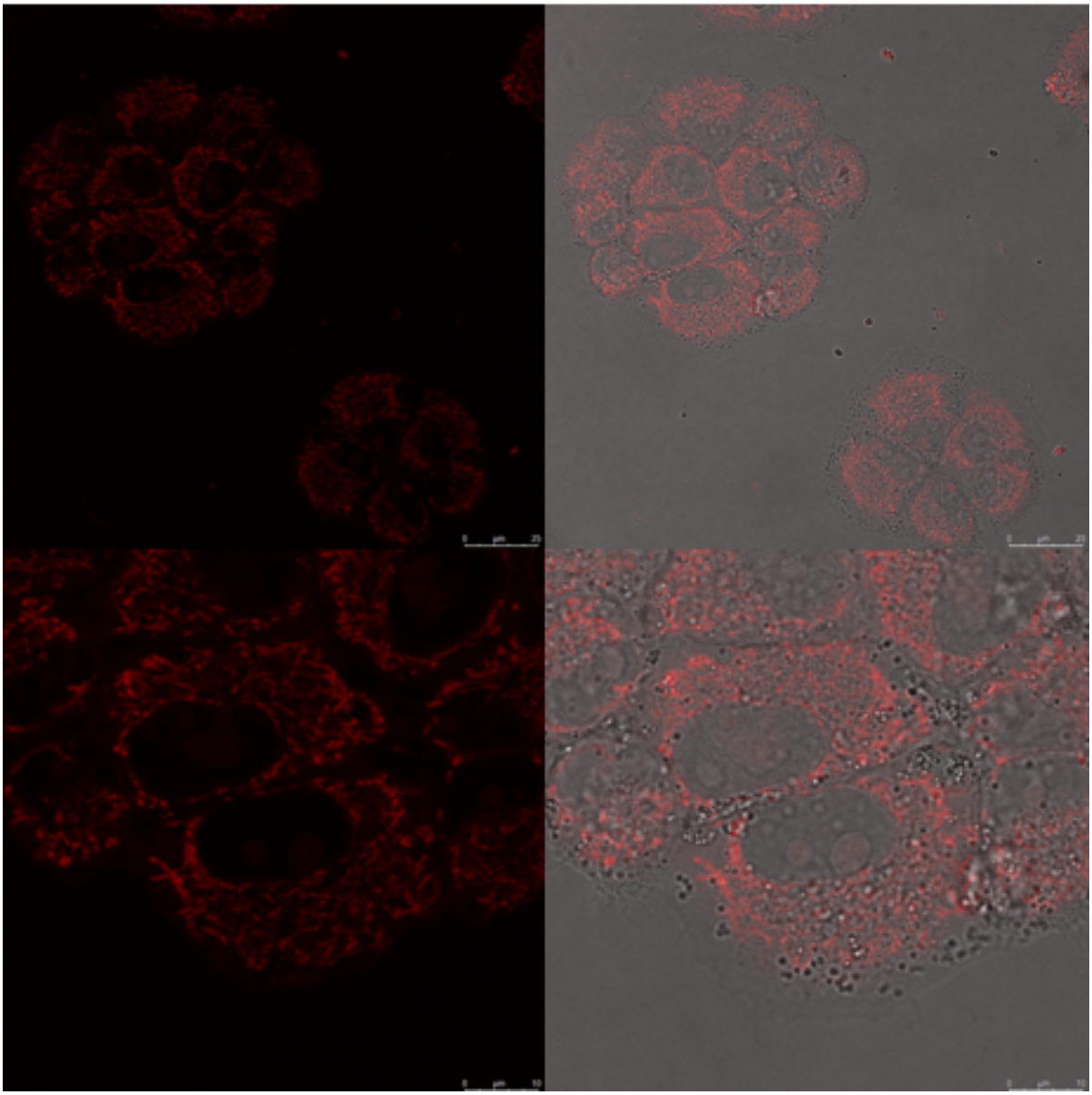

Figure S29.B) LEFT: Confocal microscopy of live cells (*c*=50000 cells/mL) taken on Leica SP8 X confocal microscope, stained with 10 μM concentration of **Q-NMe$_2$** (λ_{exc} = 500 nm, λ_{em} = 625 nm; RIGHT: overlay with the control (white light).

C)

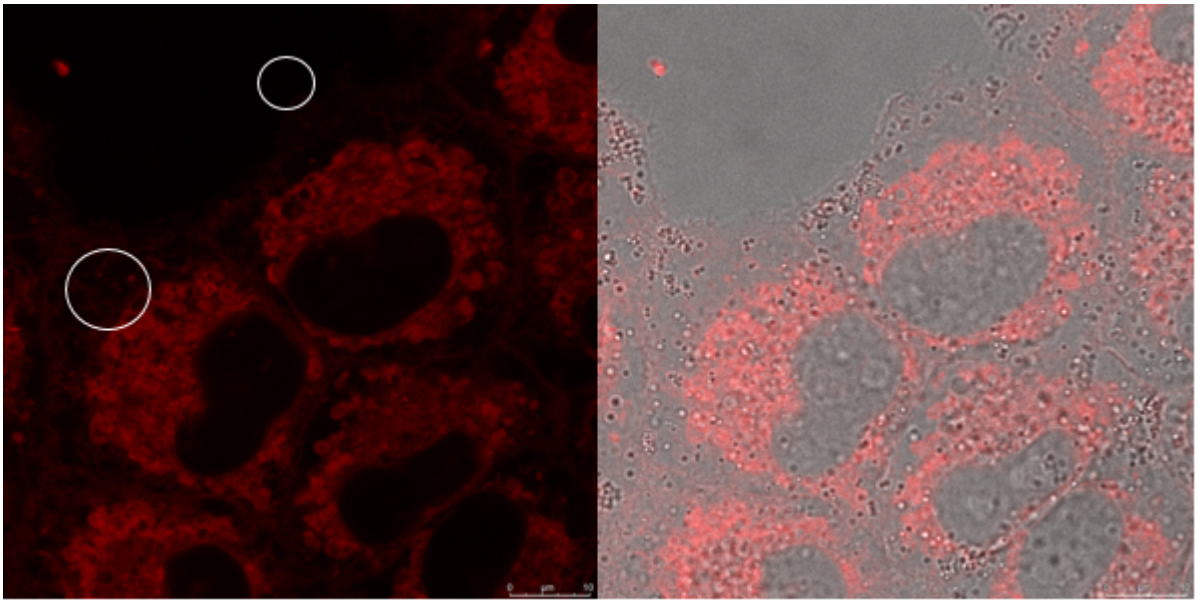

Figure S29.C) LEFT: Confocal microscopy of live cells (*c*=50000 cells/mL) taken on Leica SP8 X confocal microscope, stained with 10 μM concentration of **Q-NPh$_2$** (λ_{exc} = 488 nm, λ_{em} = 660 nm; RIGHT: overlay with the control (white light).

C')

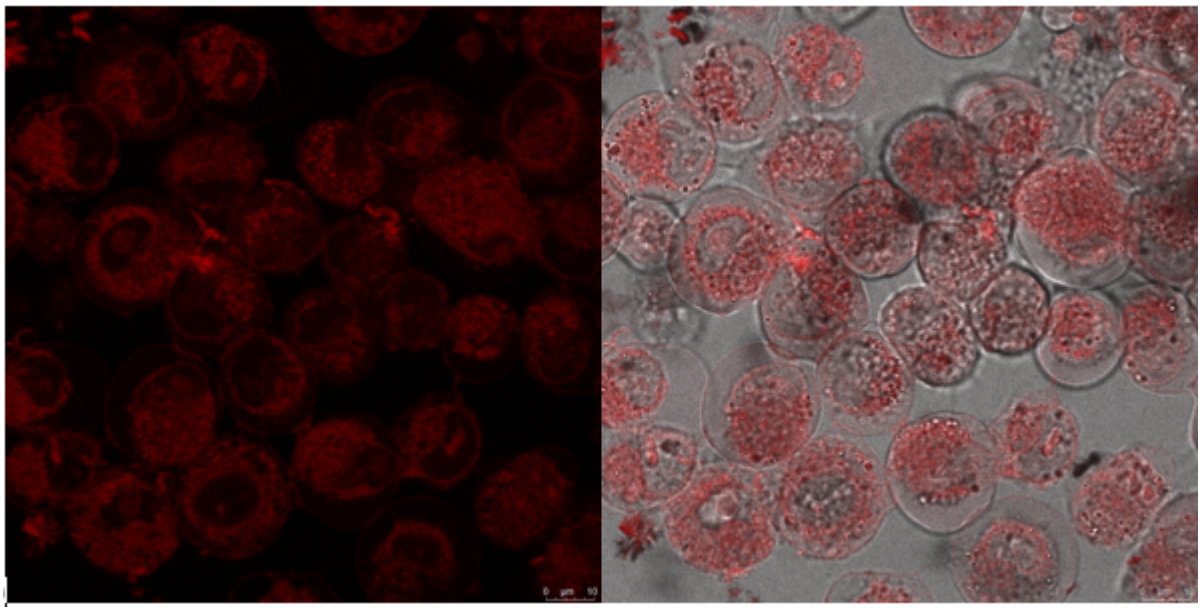

Figure S29.C') LEFT: Confocal microscopy of live cells (*c*=50000 cells/mL) taken on Leica SP8 X confocal microscope, stained with **50 μM** concentration of **Q-NPh$_2$** (λ_{exc} = 488 nm, λ_{em} = 660 nm), RIGHT: overlay with the control (white light).

D)

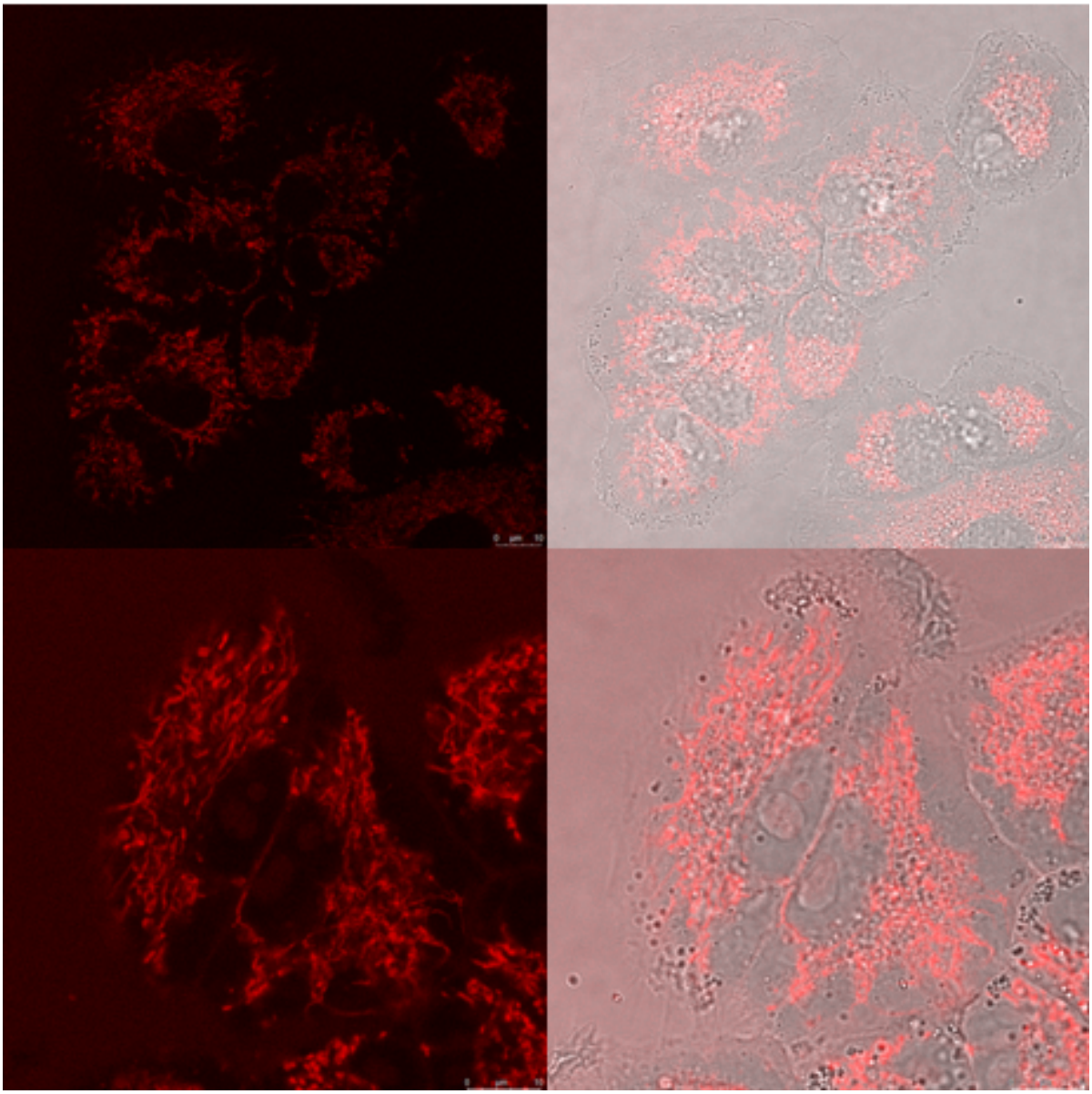

Figure S29.D) LEFT: Confocal microscopy of live cells (*c*=50000 cells/mL) taken on Leica SP8 X confocal microscope, stained with 10 μM concentration of ***p*Py-MeO-*p*Py** (λ_{exc} = 458 nm, λ_{em} = 580 nm); RIGHT: overlay with the control (white light).

E)

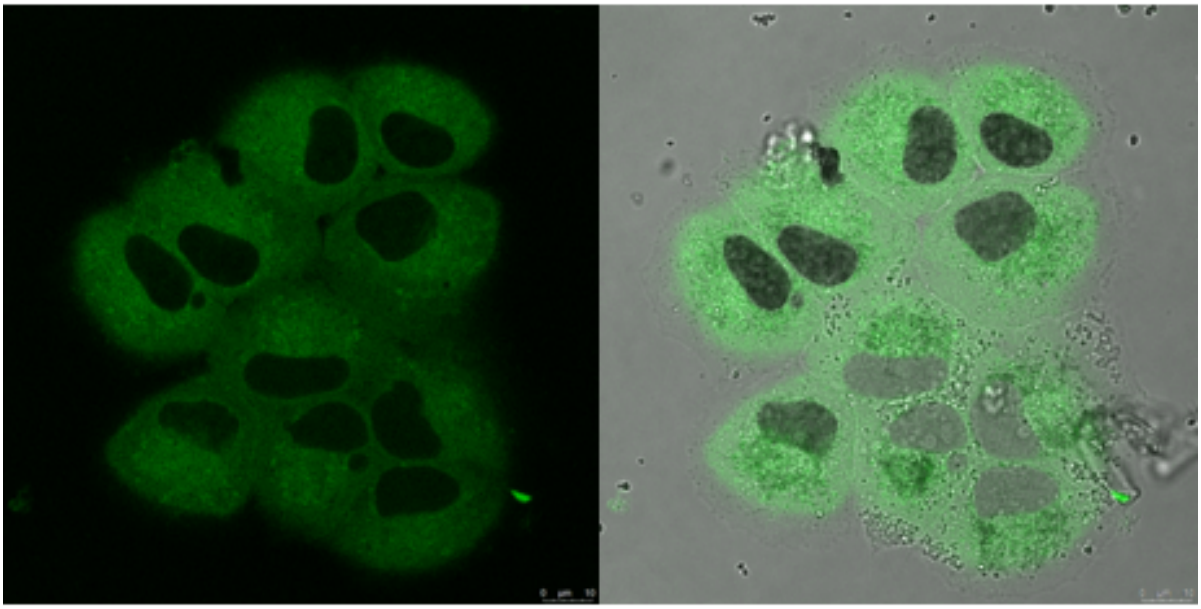

Figure S29.E) LEFT: Confocal microscopy of live cells (*c*=50000 cells/mL) taken on Leica SP8 X confocal microscope, stained with 10 μM concentration of ***o*Py-MeO-*o*Py** (λ_{exc} = 458 nm, λ_{em} = 565 nm); RIGHT: overlay with the control (white light).

NMR Spectra of ***p*Py-MeO-*p*Py** and ***o*Py-MeO-*o*Py**

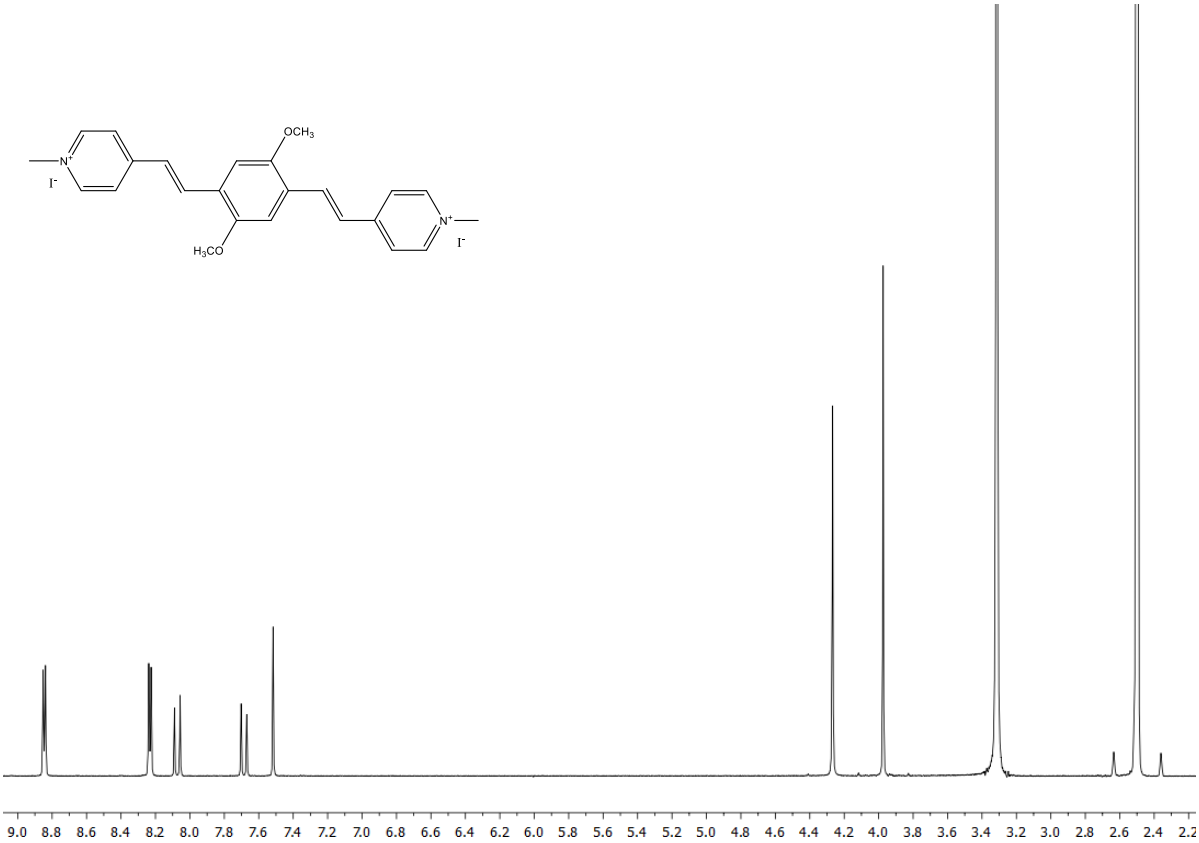

Figure S30. ^{1}H NMR spectrum of ***p*Py-MeO-*p*Py** in DMSO-d_6.

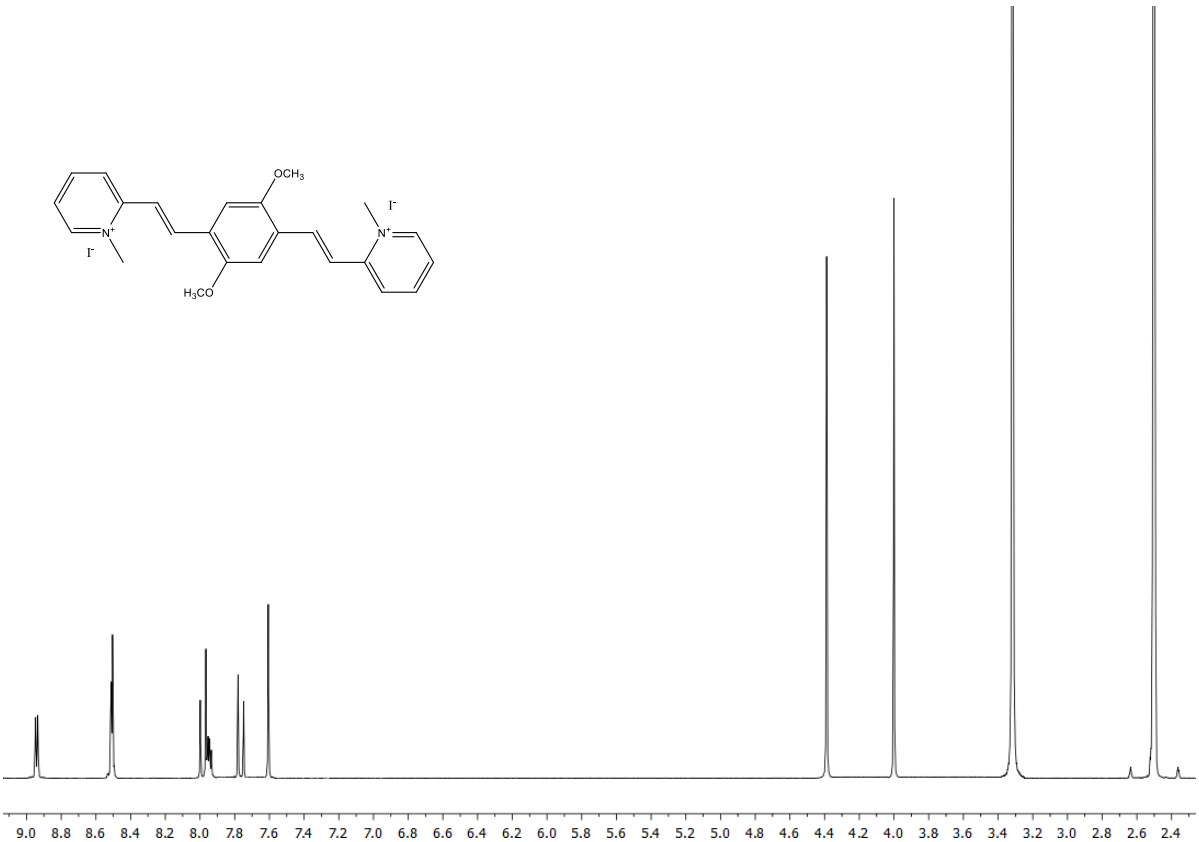

Figure S31. ^{1}H NMR spectrum of ***o*Py-MeO-*o*Py** in DMSO-d_6.

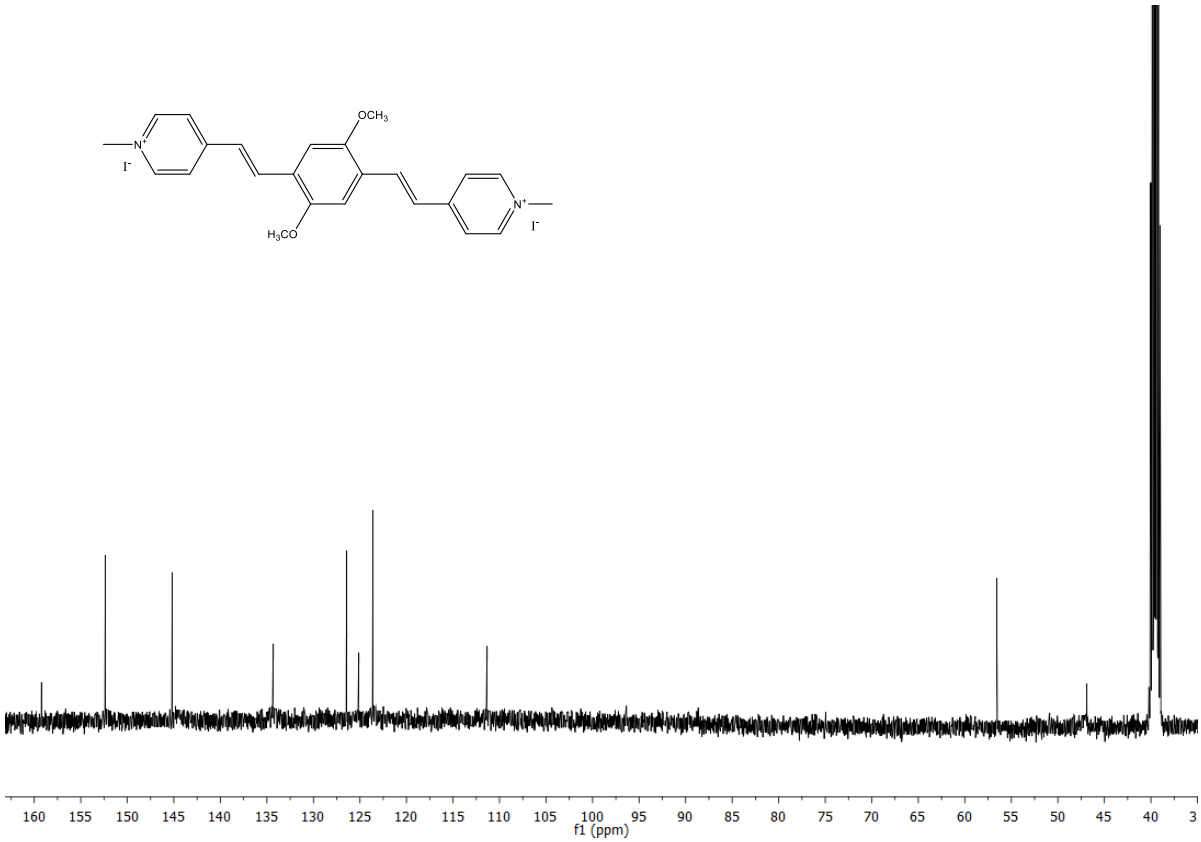

Figure S32. ^{13}C NMR spectrum of ***p*Py-MeO-*p*Py** in DMSO-d_6.

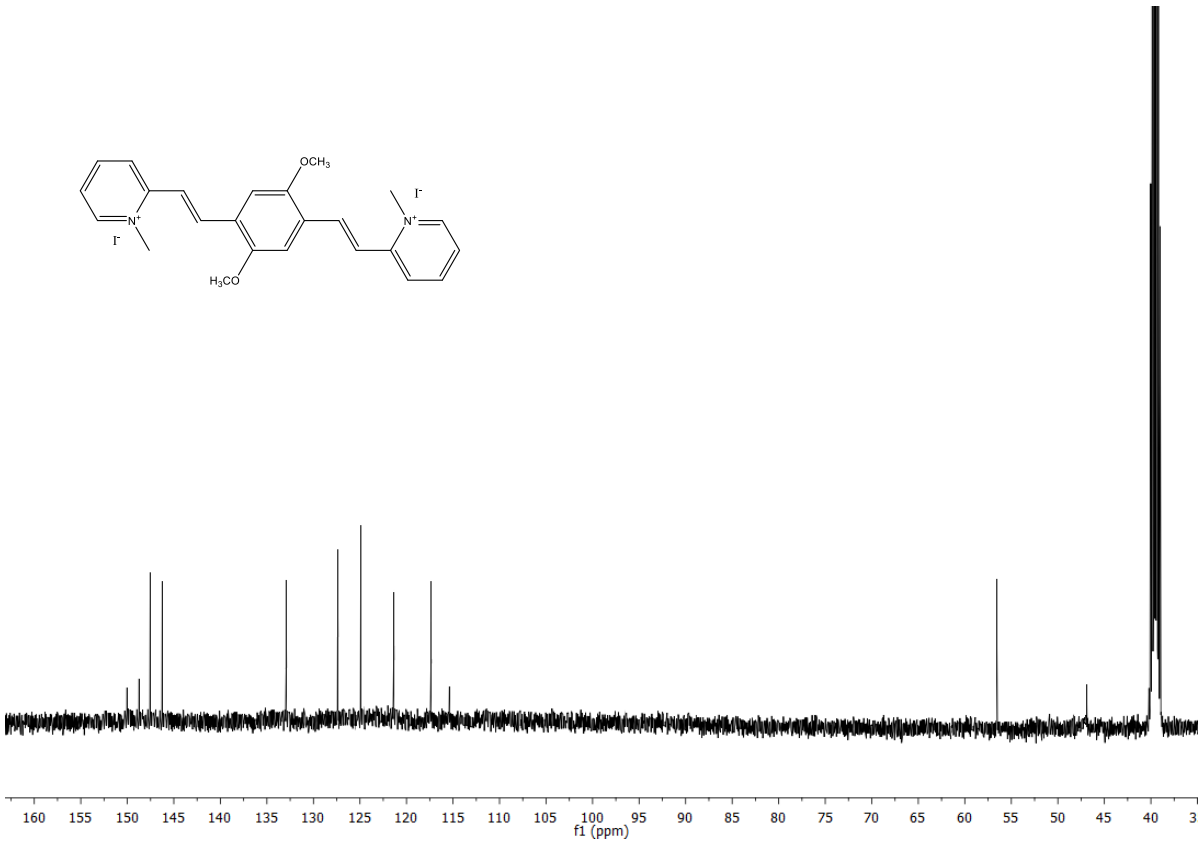

Figure S33. ^{13}C NMR spectrum of ***o*Py-MeO-*o*Py** in DMSO-d_6.

*HRMS Spectra of **pPy-MeO-pPy** and **oPy-MeO-oPy***

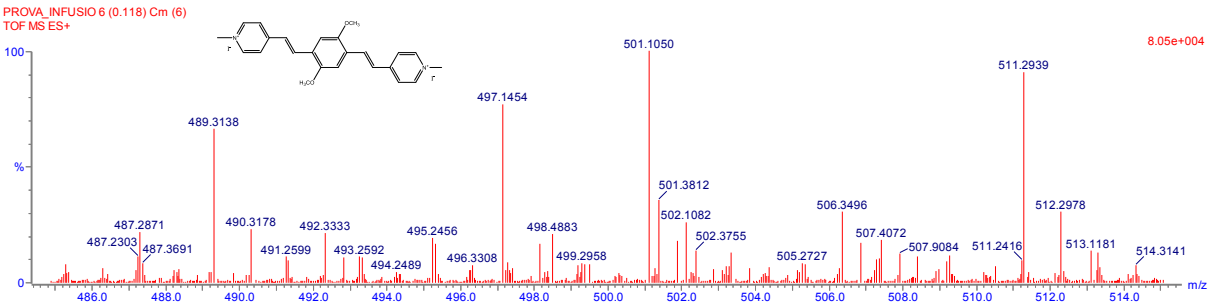

Figure S34. HRMS spectrum of *p*Py-MeO-*p*Py.

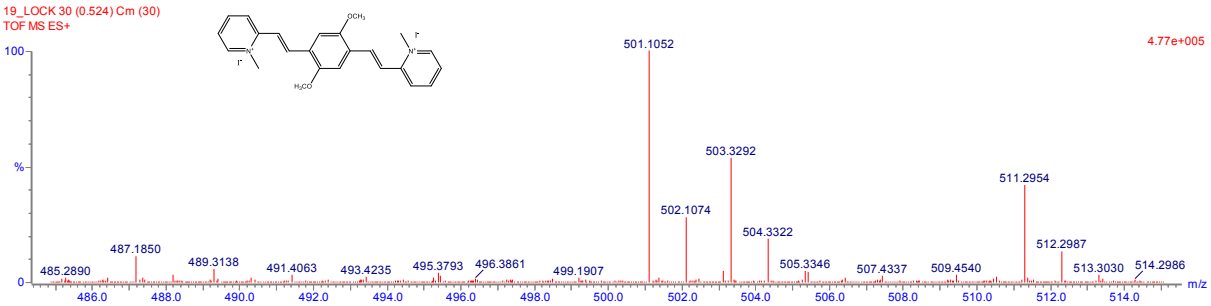

Figure S35. HRMS spectrum of *o*Py-MeO-*o*Py.

[1] Cantor, C. R., and Schimmel, P. R. (1980) Biophysical Chemistry, Vol. 3, , WH Freeman and Co., San Francisco.; Egli, M., and Saenger, W. (1983) Principles of Nucleic Acid Structure, Springer-Verlag, New York